

Unusual Adsorption Properties of Silver Adlayers on the Pt(111) Electrode Surface

N. S. Marinkovic,[†] J. X. Wang,[†] J. S. Marinkovic,[‡] and R. R. Adzic^{*,†}

Chemical Science Division, Department of Applied Science, Brookhaven National Laboratory, Upton, New York 11973, and Department of Chemistry, University of California, Davis, California 95616

Received: July 13, 1998; In Final Form: November 15, 1998

Adsorption properties of silver monolayer and bilayer deposited at underpotentials on a Pt(111) electrode were studied by means of linear sweep voltammetry, in situ surface X-ray scattering and infrared spectroelectrochemistry. Surface X-ray scattering measurements show a pseudomorphic Ag monolayer and an incommensurate expanded bilayer on Pt(111) formed at underpotentials. Unusual adsorption properties of the silver layers with respect to the bulk silver are observed. The two Ag adlayers were found to have intermediate adsorption/oxidation characteristics between those of metallic Ag and Pt surfaces with (111) orientation. The Ag monolayer has properties that facilitate adsorption of bisulfate anions and adsorption and oxidation of CO. These properties are closer to the adsorption properties of the Pt(111) surface than to those of Ag(111), which adsorbs sulfate anions and does not adsorb CO. The Ag bilayer on the Pt(111) surface adsorbs sulfate anions as Ag(111) does, but in contrast to the behavior of Ag(111), it adsorbs CO. These properties of the Ag adlayers appear to be a consequence of the charge-transfer process and the electron distribution in the Ag/Pt(111) surface.

1. Introduction

Silver adlayers formed by underpotential deposition (UPD) at metal surfaces have been investigated extensively in the past. Various in situ and ex situ techniques used for this purpose include cyclic voltammetry,^{1–4} LEED,⁵ FTIR,⁶ and X-ray scattering.^{6,7} While it has been generally accepted that the UPD process of silver deposition proceeds in two steps at platinum substrate^{2–7} involving the formation of the second layer on top of the first, the chemical characteristics of the two layers are rather unknown. It has been suggested that the properties of the two layers could be different as the formation of the first layer of silver on platinum involves a substantial mixing of the two metals.⁸ In situ scanning tunneling microscopy (STM) has shown a commensurate (1 × 1) lattice for Ag monolayer and a uniformly expanded hexagonal bilayer.⁹ As a result of the inherent drift of STM measurements, this expansion of the bilayer could not be ascertained. In a previous work,⁷ we have confirmed this anomalous structural expansion of silver bilayer on Pt(111) and proposed that such a behavior may result in unusual chemical properties of the adlayer.

Metal monolayers on foreign metal surfaces usually have properties that are strongly perturbed by the interaction with the substrate but still related to the properties of the bulk metal. The properties of the Ag adlayers found in this work can therefore be referred to as unusual, since they differ considerably from those of Ag(111). The chemical and electrochemical characteristics of the silver layers on Pt(111) are studied by means of electrochemistry, in situ X-ray scattering, and FTIR spectroscopy.

2. Experimental Section

All solutions were prepared from chemicals of the highest purity available obtained from Alpha and MilliQ-UV-plus water

(Millipore). The reference electrode was always a reversible hydrogen electrode in the corresponding solution. Platinum single-crystal electrodes of (111) orientation (Metal Crystals and Oxides, Cambridge, England) were polished with diamond pastes down to 0.3 μm . Before each experiment, the electrodes were heated in a propane–air flame for ~ 5 min and cooled to room temperature in a hydrogen stream. The electrode was protected by a water droplet while being transferred to the electrochemical cell. The cleanliness of the solutions and the quality of surface ordering were checked before each measurement by linear sweep voltammetry. The same technique was used to obtain first information on the formation of silver layers on the Pt(111) electrode in a solution of 0.05 M H_2SO_4 + 1 mM Ag_2SO_4 .

Surface X-ray scattering (SXS) measurements were carried out at the National Synchrotron Light Source at Brookhaven National Laboratory, at the beam line $\times 22\text{B}$. The description of the electrochemical SXS technique and the cell design has been presented earlier.¹⁰ For convenience, a hexagonal coordinate system was chosen, in which the reciprocal space wave vector is $Q = (a^* \cdot b^* \cdot c^*) \cdot (H, K, L)$, where $a^* = b^* = 4/(3\sqrt{3})\pi a$, $c^* = \sqrt{3}/3 \pi a$ and L is parallel to the surface normal.¹⁰

The cell for in situ infrared spectroelectrochemical measurements and the optical path were described previously.^{11,12} Both ZnSe and CaF_2 hemispheres were used as IR windows in this study. The Mattson RS-10000 spectrometer and a PAR 273 potentiostat were computer controlled using a program designed to set the potential of the working electrode alternatively to the sample or the reference potential for the working electrode prior to sample acquisition. The reference potential was constant and chosen to be in the potential region of formation of the second silver layer in the corresponding electrolyte. A total of 4096 scans were coadded in cycles of 128 scans each. Throughout the study, 8 cm^{-1} resolution was used. The subtractively normalized interfacial Fourier transform infrared (SNIFTIR)

[†] Brookhaven National Laboratory.

[‡] University of California.

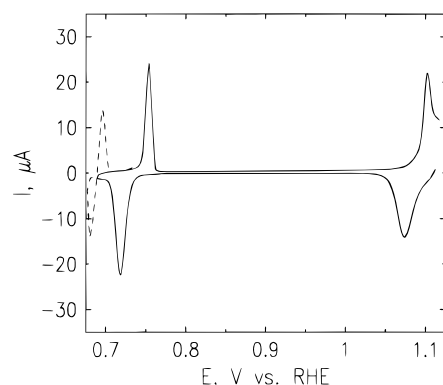


Figure 1. Voltammetry curve of Pt(111) in 0.05 M H_2SO_4 + 1 mM Ag^+ . Sweep rate = 2 mV s^{-1} . Dashed line shows the onset of bulk silver deposition.

spectra, $-\Delta R/R$ are given in the figures, with the positive-going bands representing a gain of a particular species at the sample potential relative to that at the reference.

3. Results and Discussion

3.1. Voltammetry Measurements of Ag Deposition on Pt(111). Figure 1 shows a typical cyclic voltammogram for the silver deposition at a Pt(111) electrode in 0.05 M H_2SO_4 + 1 mM Ag^+ . In this electrolyte, the instability problem of Pt(111) at high anodic potentials is overcome as the strong adsorption of bisulfate anions prevents the oxidation of Pt at potentials of Ag monolayer dissolution. The first silver adlayer forms in the region 1.15–1.05 V, and the second layer deposits on top of the first at 0.73 V in a narrow potential region, 50 mV positive of the reversible potential of the Ag/Ag^+ electrode reaction. The charges under each of the two voltammetric peaks are 249 and $261 \mu\text{C}/\text{cm}^2$ for the peaks at 1.08 and 0.73 V, respectively. This is close to $240 \mu\text{C}/\text{cm}^2$, which is the expected value for a full monolayer of Ag at the Pt(111) surface. In a wide potential region between the two silver deposition processes, only a double layer charging is observed in the voltammogram. This potential region was investigated further by in situ SXS and FTIR techniques.

3.2. In situ SXS Measurements. The surface structures of the silver adlayers electrodeposited at underpotentials were carried out by SXS. In-plane scans along the $(0, K, 0.3)$ axis at three potentials, viz., 1.1, 0.91, and 0.71 V for Pt(111) in 0.05 M H_2SO_4 + 1 mM Ag^+ are given in Figure 2. These potentials correspond to the Ag-free Pt, Ag monolayer and Ag bilayer. Both the Ag-free Pt(111) and Ag monolayer show only diffraction peaks at integer positions. The absence of the peaks at noninteger positions for the scans taken at 0.91 V is expected for silver atoms forming a commensurate (1×1) monolayer. The decrease of the $(0, 1, 0.3)$ peak intensity at 0.91 V, in comparison to that at 1.1 V, clearly indicates that the Ag atoms reside in 3-fold hollow sites of the Pt lattice, as only in that case a destructive interference between the atoms of Pt substrate and the adlayer is expected.

The deposition of the second layer at 0.71 V produces a diffraction pattern shown in the inset of Figure 2. The presence of the reflections at noninteger positions in reciprocal space indicates the formation of an incommensurate adlayer with a lattice constant larger than that of Pt, i.e., $a_{\text{Pt}}/0.94$. On the basis of these experiments, a model for the Ag adlayers on Pt(111) is drawn in Figure 3, together with the models for Pt(111) and Ag(111). A contraction and expansion of the adlayers' lattice constants with respect to that of bulk silver is observed for the

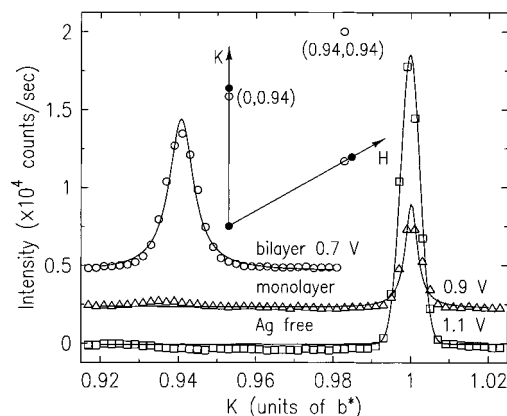


Figure 2. In-plane diffraction scans along the $(0, K, 0.3)$ axis from Pt(111) in 0.05 M H_2SO_4 + 1 mM Ag^+ at different potentials. Spectra are offset for clarity. Solid lines are fitted to a Lorentzian shape. Inset shows the in-plane diffraction pattern taken at 0.71 V.

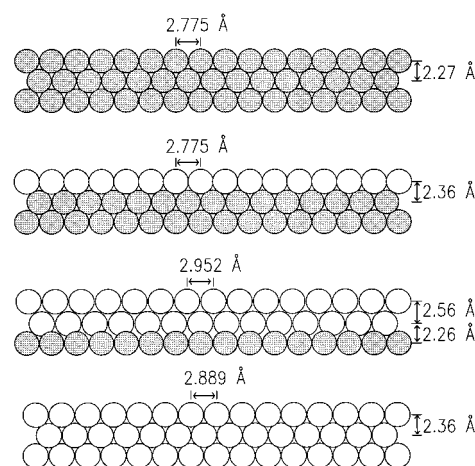


Figure 3. Models for the Pt(111) surface (a), Ag monolayer (b), and bilayer (c) underpotentially deposited on the Pt(111) substrate and the Ag(111) surface (d) along the $(1, 0)$ substrate axis. Lattice spacings for the monolayer and bilayer are measured as in ref 7 and compared to those of bulk platinum and silver.

monolayer and bilayer, respectively. The two Ag layers in the bilayer are mutually commensurate but incommensurate with the Pt substrate. This unusual expansion of the electrochemically deposited Ag bilayer appears to result from the repulsion among Ag atoms due to a large electron transfer from Ag to the more electronegative Pt substrate, as discussed in detail elsewhere.⁷ It is therefore anticipated that the silver adlayers may have interesting chemical and electrochemical properties different from that of bulk metallic silver, as discussed in the forthcoming sections.

3.3. In situ FTIR Measurements. **3.3.1. Anion Adsorption on the Ag Bilayer.** Figure 4 shows the SNIFTIR spectra of adsorbed anions from 0.05 M H_2SO_4 on the Ag monolayer on Pt(111), obtained by using both CaF_2 (Figure 4a) and ZnSe (Figure 4b) hemisphere windows. The spectra in Figure 4a were taken 50 mV apart, starting at 0.8 V. Reference scans were taken at 0.7 V, in the bilayer potential region. A characteristic, bipolar-shaped band is observed in the spectra in the potential region between 0.8 and 1.05 V, with a negative-going lobe centered at 1178 cm^{-1} and a positive-going lobe centered around 1205 cm^{-1} , which shifts in frequency as the potential is made more positive. The bipolar shape of the band implies that there is a difference in the adsorption of sulfate and/or bisulfate at the electrode surface at the sample potential of Ag monolayer with

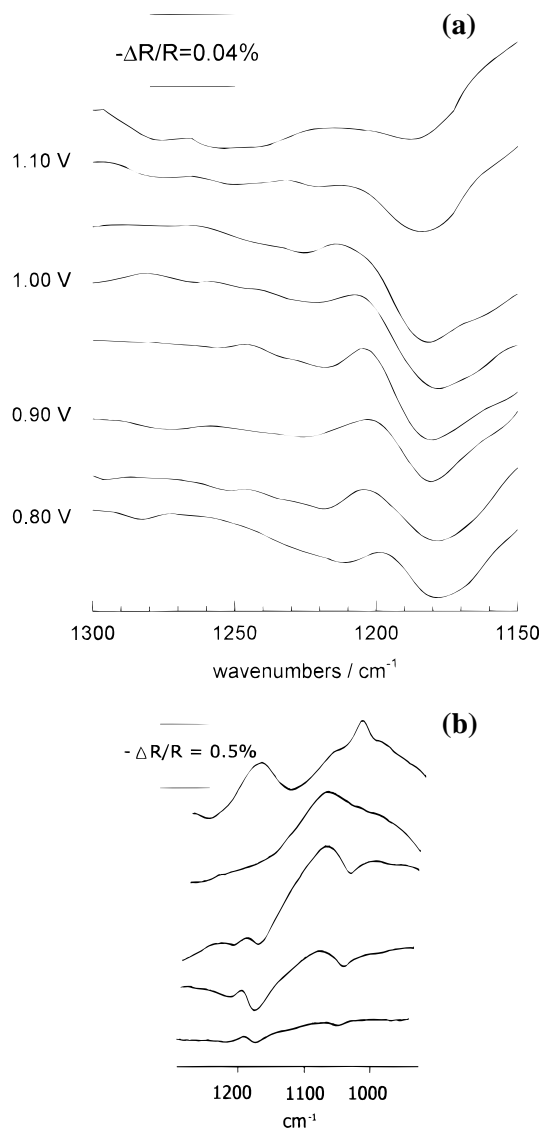


Figure 4. SNIFTIRS spectra of sulfuric acid anions adsorbed on silver monolayer and bilayer deposited on Pt(111) substrate from 0.05 M $\text{H}_2\text{SO}_4 + 1 \text{ mM Ag}^+$. Spectra are taken at 50 mV apart, starting at 0.8 V (a), and 100 mV apart, starting at 0.8 V (b). Reference scans are taken at 0.7 V in both experiments. CaF_2 (a) and ZnSe (b) hemispheres are used as the IR window. 4096 scans with 8 cm^{-1} resolution are coadded. Spectra are offset for clarity.

respect to that at the reference where Ag bilayer is formed. This behavior will be further analyzed below.

Bipolar character of a SNIFTIRS band is a quite common phenomenon. It is usually explained in terms of a potential-induced change in band frequency upon the adsorption of the molecule at the electrode surface. As a result of the subtractive nature of the spectral presentation, the band in the spectrum taken at the reference potential becomes negative, whereas that taken at the sample potential becomes positive. The most often studied case is the adsorption of CO molecule on platinum surface,¹³ where the change in frequency is explained by the (potential-dependent) extent of d-electron transfer from the metal to the CO antibonding orbital.¹⁴ The frequency change of a molecular vibration can be also induced by the different interaction of the molecule with the electrode surface upon its reorientation at potentials around the point of zero charge, as was found for dimethylacetamide adsorption at gold,¹⁵ water and acetonitrile adsorption at platinum,^{16,11} etc. However, it is also possible to observe a bipolar-shaped band if there are two

different spectral bands, close in frequency but with opposite potential dependence. The discussion that follows indicates that the last phenomenon applies to the present case of anion adsorption on Ag adlayers.

It has been shown in a recent work that sulfate anions are the predominant species adsorbed at the Ag(111) electrode surface in acidic and neutral solutions.¹² The sulfate adsorption at the electrode surface produces a band at $\sim 1170 \text{ cm}^{-1}$ that shifts to higher wavenumbers as the potential is made more positive, with a rate of $60 \text{ cm}^{-1}/\text{V}$. The highest frequency of the band, 1182 cm^{-1} , appears in the spectrum taken at 0.6 V vs RHE, i.e., just before the onset of silver dissolution in 0.05 M H_2SO_4 .¹² In the present case, the negative-going band is observed at $\sim 1178 \text{ cm}^{-1}$. This frequency is in the range of the bands that appear for the Ag(111)–sulfate system at different potentials and is lower than the frequency of the bisulfate ion in the solution ($\sim 1195 \text{ cm}^{-1}$). Therefore, it seems reasonable to ascribe the band to strongly blue-shifted $\nu(\text{SO}_4^{2-})$ mode of sulfate anions adsorbed at the silver bilayer.

When the potential is shifted to higher values, the silver bilayer is dissolved and the sulfate anions adsorbed on top of silver atoms also leave the surface. This is observed from the strong, positive-going band at $\sim 1110 \text{ cm}^{-1}$ for the sulfate anions in all spectra in Figure 4. The surface of the platinum electrode covered with silver monolayer has to be quickly covered by either (or both) sulfate or bisulfate species. To distinguish which type of anion is predominantly adsorbed, one could try to analyze in situ FTIR spectra obtained in different solution pH, thus changing the sulfate/bisulfate ratio in the bulk of the solution. This method has been used to identify the predominant species adsorbed on Pt(111) as bisulfate or the sulfate–hydronium ion pair.¹⁷ This procedure is not easily applicable to the case of Ag UPD at Pt(111) since the change of pH to higher values shifts negatively the onset of PtOH formation on which silver cannot adsorb. Therefore, one could conclude about predominant species only from the IR results obtained in low pH values. Nevertheless, the discussion that follows strongly suggests that the bisulfate is the predominant species adsorbed at the silver monolayer.

3.3.2. Anion Adsorption on the Ag Monolayer. The IR spectrum of bisulfate ion in a solution is characterized by a doubly degenerate SO_3 stretching mode at 1195 cm^{-1} and a totally symmetric SO_3 stretch at 1050 cm^{-1} .¹⁸ It has been proposed that the latter band shifts strongly to higher wavenumbers upon the adsorption of bisulfate at the Pt(111) electrode surface, producing the potential-dependent, positive-going band at $\sim 1250 \text{ cm}^{-1}$. The adsorption process also produces a negative-going band at 1050 cm^{-1} , due to the conversion of solution-phase bisulfate ions to adsorbed species.¹⁹

In the present study, the potential-dependent, positive-going band at $\sim 1205 \text{ cm}^{-1}$ in Figure 4a is likely to be due to adsorbed bisulfate, because the bulk HSO_4^- concentration in 0.05 M H_2SO_4 is about 5 times higher than that of sulfate. To confirm this, spectra were taken using a ZnSe hemisphere to extend the spectral range beyond the cutoff of the CaF_2 window. In addition to the two bands due to adsorbed sulfate and bisulfate species observed in the spectra collected using CaF_2 window, two more bands at 1110 and 1050 cm^{-1} can be seen in Figure 4b. The positive-going band at 1110 cm^{-1} is ascribed to the increase in concentration of sulfate anions in the diffuse part of the double layer. It appears as a strong and positive band in the spectra taken at all sample potentials. The other band at 1050 cm^{-1} is ascribed to the bisulfate species in the solution. Its potential behavior is more complex; it is negative-going at sample

potentials lower than 1.0 V but changes its sign as the potential is further increased. The potential behavior of these two solution bands provides the information on the type of anions predominantly adsorbed on the Ag monolayer. If one assumes that the sulfate anions are adsorbed at the electrode surface both at the bilayer and the monolayer of silver, the change in anion concentration in the double layer upon dissolution of the Ag bilayer would reflect the diffusion of anions from the bulk of the solution into the double layer to compensate the increase of the positively charged silver cations. In that case, the bands for both sulfate and bisulfate ions in the solution should be positive-going. Figure 4b shows that such a behavior is not observed at sample potentials at which the Ag monolayer is stable, i.e., below 1.07 V (see the voltammetry curve in Figure 1). On the other hand, if bisulfate ions are predominantly adsorbed at the silver monolayer, upon the Ag bilayer dissolution, the spectrum should be composed of the positive-going band for sulfate ions in the double layer and the negative-going band for bisulfate, with the latter representing the loss of bisulfate ions in the diffuse part of the double layer due to adsorption at the electrode surface. Figure 4b shows precisely this behavior; the band representing the loss of the bisulfate ions in the solution at 1050 cm^{-1} always accompanies the positive-going band for the adsorbed bisulfate ions at $\sim 1205\text{ cm}^{-1}$.

The cyclic voltammogram given in Figure 1 shows that the desorption process of silver monolayer commences above 1.05 V. The increase of the positively charged Ag ions in the double layer has to be compensated by the diffusion of anions into the diffuse part of the double layer. As expected, this process produces positive-going bands in the spectra for both sulfate and bisulfate ions in the solution. The two topmost spectra in Figure 4b, taken at 1.1 and 1.2 V, indeed show a manifold of characteristic bands for the solution spectrum of sulfuric acid produced by diffusion of these anions.

Figure 5a shows the potential dependence of the frequency for the bisulfate species adsorbed at the silver monolayer. In a relatively wide potential range, there is a linear dependency of the ν_{\max} (E) plot with a slope of $33\text{ cm}^{-1}/\text{V}$. This slope is considerably smaller than that found for sulfate on Ag(111) and bisulfate on the Pt(111) surface.^{12,19} Therefore, one concludes that different chemical properties of the bimetallic surface change the adsorption behavior of the sulfuric acid anions. The potential dependence of integrated intensity of the band for bisulfate adsorbed on silver monolayer is shown in Figure 5b. In a relatively wide potential region, a linear dependence of the coverage is obtained, indicating a repulsive interaction among the adsorbed anions. The profile of the pseudoisotherm resembles the shape of that observed for sulfate adsorption on the Ag(111) electrode.¹² This coincidence is surprising as different types of anions are adsorbed on Ag(111) and Ag monolayer and points out further the unusual chemical properties of the metal adlayer.

Sulfate adsorption on Ag(111) and Au(111) has been extensively studied, both experimentally and by ab initio calculations. On the basis of the vacuum spectroscopic data, Mrozek et al.²⁰ pointed out that the electron density on sulfur increases upon adsorption on Au(111) and attributed this phenomenon to a back-donation into some unfilled electronic orbitals on the sulfate adsorbate. Ab initio calculations of sulfate adsorption on Au and Ag metals with (111) orientation confirmed this observation. They also indicated that sulfate mainly interacts with the s and p bands of the metal, toward which there is a charge transfer of about 0.4 electrons.²¹ Sulfate

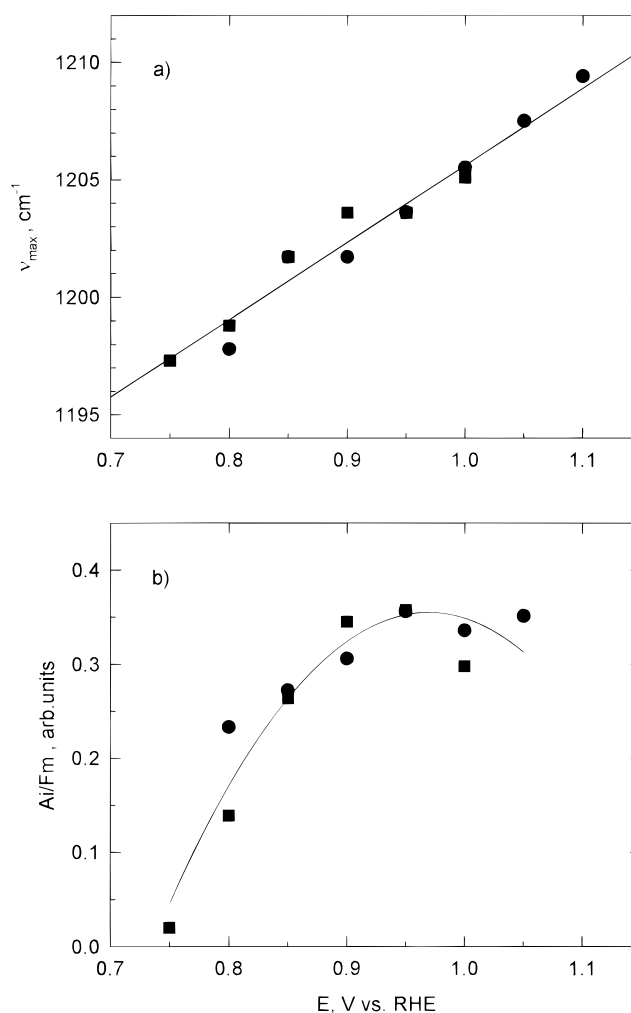


Figure 5. Potential dependence of frequency (a) and normalized integrated band intensity (b) for the positive-going bisulfate band centered around 1178 cm^{-1} for two separate data collections. For normalization procedure see ref 12.

ions are therefore only partially discharged, and that could be the origin of the large repulsive interactions among the adsorbates observed experimentally.^{12,22}

Electronic properties of bimetallic surfaces can be very different from those of the substrate and the bulk adlayer. Work function measurements^{23,24} show a large charge transfer from Ag to the substrate, leaving a small positive charge on the adlayer. As the electron density in the Ag adlayer decreases by about 0.15 e/atom,²⁵ the repulsion among the ion cores increases. Therefore, the Ag bilayer is expanded with respect to bulk silver, as found in the present work. A comparison of the atomic orbital populations for the Ag/Pt₉ and Ag/Ag₉ indicates that the Ag(s,p) to Pt charge transfer is accompanied by Pt to Ag(d) and Ag(s,p) to Ag(d) electron transfers. The noble metal behaves as an (s,p) electron donor and d-electron acceptor. For the Pt(111) substrate, bimetallic bonding induces a reduction in the Pt(5d) population and a Pt(5d) to Pt(6s,6p) rehybridization.²⁵

The above discussion indicates that both platinum and silver metal are affected upon formation of adsorbed silver monolayer. The electron transfer from the Ag s and p orbitals to the platinum substrate apparently decreases the adsorption affinity toward sulfate, because this anion mainly interacts with those orbitals.²¹ In addition, the orbital rehybridization increases the ability of the Ag monolayer to adsorb CO, as suggested for the metal–gas interface²⁵ and confirmed by SNIFTIRS measurements for the electrochemical system, presented below. Therefore, it

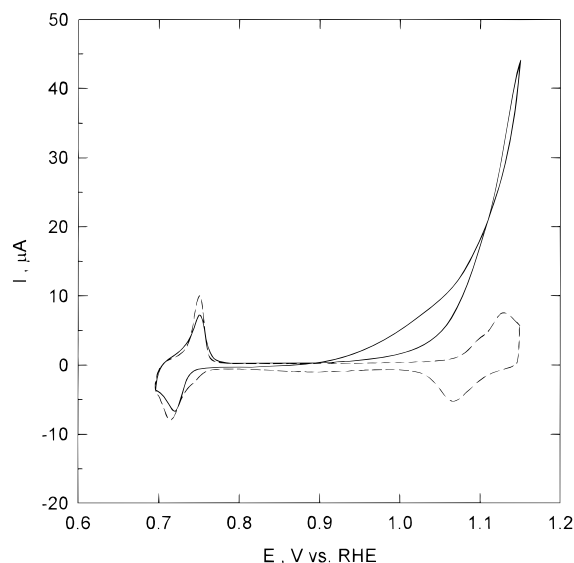


Figure 6. Voltammetry curves of CO oxidation on the Ag monolayer deposited on Pt(111) in a CO-saturated solution of 0.05 M H_2SO_4 + 1 mM Ag^+ (full line) and the curve in the absence of CO (dashed line); sweep rate = 2 mV s^{-1} .

appears that the adsorption properties of the silver monolayer adsorbed at underpotentials on Pt(111) are similar to those of d-metals with the (111) surface orientation. Since it has been shown that the Pt(111) surface adsorbs bisulfate,¹⁹ the adsorption of this anion on the Ag monolayer with increased d-orbital character is not surprising. Also, the excess of positive charge on the Ag adlayer could be used to interpret the relatively low slope of the ν_{max} (E) plot for bisulfate on the Ag monolayer. On the other hand, the sulfate adsorption on both bulk Ag(111) and on Ag bilayer deposited on Pt(111) implies that the latter structure is commencing to acquire some chemical properties similar to those of Ag(111), which in turn differ from those of the Ag monolayer.

3.3.3. Adsorption and Oxidation of Carbon Monoxide. CO adsorption on metal surfaces is usually explained in terms of the Blyholder model, which involves a weak electron transfer from the 5σ CO orbital onto the substrate, followed by a stronger back-donation from the metal d-band into the $2\pi^*$ CO orbital.¹⁴ The consequence of this process is that the frequency of the adsorbed CO at metal substrates is lowered from the gas-phase value of 2138 cm^{-1} . In the case of the sp metals such as Ag, the back-donation is small because of the low-lying d-band so that CO is usually considered to be physisorbed. Only an indication of a weak chemisorption of CO is found on silver metal.²⁶ Recent vibrational studies of CO adsorbed on silver multilayers on Pt substrate at the metal–gas interface indicate that Ag–Pt interaction enhances the strength of the Ag–CO bond and that the intensity of the CO band decreases with an increasing number of Ag monolayers.^{27,28} This is explained in terms of the increase in d-electron population at the Ag–Pt(111) surface,²⁵ as the valence d orbitals are much more suitable for bonding interactions with CO than the (s,p) orbitals. The increase in d population of the noble metal causes an enhancement in the bonding interactions between the noble metal d orbitals with CO ($2\pi^*$) orbitals, increasing the π back-donation and the strength of the Ag–CO bond.²⁵

Figure 6 shows the cyclic voltammogram of CO oxidation on the Ag monolayer deposited at a Pt(111) electrode. In the anodic scan, CO oxidation commences at 0.9 V and continues throughout the whole potential range beyond. A considerable current is obtained before the onset of the silver monolayer

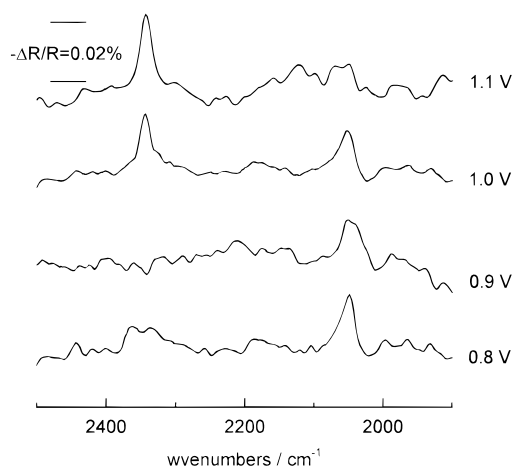


Figure 7. SNIFTIR spectra of CO adsorption and oxidation on the silver monolayer deposited on Pt(111) in CO-saturated solution of 0.05 M H_2SO_4 + 1 mM Ag^+ . Sample scans are taken 100 mV apart, starting at 0.8 V. Reference scans are taken at 0.7 V. CaF_2 hemisphere is used as the IR window. 768 scans with 8 cm^{-1} resolution are coadded. Spectra are offset for clarity.

dissolution (at about 1.07 V). A rapid increase in the oxidation current beyond this potential indicates that CO is oxidized on the Ag-free sites. The CO oxidation in the cathodic direction proceeds in a somewhat wider potential region and with higher currents. Sizable anodic currents associated with the oxidation of CO in both cathodic and anodic scans indicate a considerable rate of its adsorption on the Ag monolayer on Pt(111).

There are no data for CO adsorption and oxidation on Ag(111) surface. The potentials of CO oxidation on the Ag monolayer on Pt(111) cannot be achieved with a metallic silver electrode because of its dissolution above 0.7 V. This is confirmed by in situ FTIR spectroscopy. SNIFTIR spectra of a Ag(111) electrode immersed in a 0.05 M H_2SO_4 solution saturated with carbon monoxide show no bands for CO adsorption or oxidation in the spectra taken in the potential interval where the Ag electrode is stable. The spectra taken at all potentials up to 0.65 V are essentially featureless in the region 2500–1800 cm^{-1} and therefore not presented in this work.

Figure 7 shows the SNIFTIR spectra of CO adsorption and electrooxidation at the silver adlayer at Pt(111), obtained in a cell with a CaF_2 window. The reference spectrum is taken at 0.7 V, i.e., at the potential of bilayer formation, and the sample scans are taken in the region from 0.8 to 1.1 V, incremented by 0.1 V. A small, yet distinguishable bipolar band is observed in the bottom three spectra. It consists of a negative-going lobe at 2020 cm^{-1} and a positive-going one at $\sim 2050 \text{ cm}^{-1}$ that shifts to higher wavenumbers as the potential of the electrode is made more positive. According to the above discussion, it follows that the negative-going band represents the linearly bonded CO to the silver bilayer and the positive-going lobe is a consequence of the CO bond to the silver monolayer. One should also note that the relative intensity of the two lobes is different, with the positive-going lobe being higher. This is in agreement with the results of Ito et al. who found that the intensity of the infrared CO band is small for a multilayer Ag film on Pt(111).²⁸

The stretching frequency of the positive lobe of the bipolar band shown in Figure 7 shifts to the higher frequencies with a rate of about 15 cm^{-1}/V with increasing potential. This rate is smaller than the one found for the adsorption of CO at Pt, for which a usually reported value is about 30 cm^{-1}/V .²⁹ It is also noteworthy that the frequency of the positive lobe for the Ag/Pt(111)–CO system of $\sim 2050 \text{ cm}^{-1}$ is lower than that found

for Pt(111)–CO (2070 cm^{-1}). This behavior is unusual, as the frequency of the CO band is inversely proportional to the amount of electron back-donation from the d orbitals of the substrate to the $2\pi^*$ CO orbital. Further work is needed to clarify this phenomenon.

At the potentials equal to or higher than 1.0 V, a sharp, positive-going band appears at 2343 cm^{-1} . This band is assigned to the solution phase CO_2 , formed as the oxidation product of CO adsorbed at the electrode surface. One should note that the shape of the band differs from that of gaseous CO_2 , which appears as a doublet. As the electrode potential reaches 1.1 V, the band for CO_{ad} is almost completely absent from the spectra and only the band at 2343 cm^{-1} is visible.

4. Conclusions

On the basis of the results presented above, it appears that there is a gradual change of the adsorption and electrocatalytic properties of the silver adlayers deposited on the Pt(111) electrode. The bulk platinum with (111) orientation is known to readily adsorb and oxidize CO molecule. The fact that the (1×1) commensurate Ag monolayer also has that capability points out on a large charge electron transfer from Ag to Pt and to subsequent electron redistribution within the monolayer. Since it has been shown that d orbitals are involved in the CO adsorption, the electronic properties of the monolayer with increased d-orbital electron population are closer to Pt(111) than to the bulk silver. An interesting implication of this conclusion is that d orbitals appear to be involved in bonding between bisulfate species and the Pt electrode, since both Pt(111) and Ag monolayer deposited on Pt(111) adsorb HSO_4^- ions. On the other hand, the deposition of the second Ag layer on Pt(111) substrate considerably changes the structure of such a surface with respect to that of Ag monolayer. The two silver layers are commensurate with each other but expanded and incommensurate with Pt. Increased charge transfer from Ag bilayer to Pt is probably the cause of this unusual expansion. However, the electron back-donation from Pt to the d orbitals of Ag bilayer seems to be lower than that of the monolayer, possibly because there are two layers that share the same amount of electrons donated from the platinum substrate. The Ag bilayer appears to have increased d-electron population with respect to that of bulk silver, yet smaller than that of the monolayer. Consequently, the Ag bilayer is still capable of adsorbing CO, unlike the metallic silver. However, the s and p orbitals of the Ag bilayer appear to be less perturbed than those of the monolayer. Consequently, the Ag bilayer surface adsorbs sulfate ions, like the Ag(111).

Acknowledgment. This research was performed under the auspices of the U.S. Department of Energy, Chemical Sciences and Materials Sciences Division, under Laboratory Energy Research Program DE-AC 02-98CH10886.

References and Notes

- (1) Candle, S. H.; Bruckenstein, S. *Anal. Chem.* **1971**, *43*, 1858.
- (2) Hammond, J. S.; Winograd, W. *J. Electroanal. Chem.* **1977**, *80*, 123.
- (3) Ocon, P.; Herrasti, P.; Palacio, C.; Vela, M. E.; Salvarezza, R. C.; Vasquez, L.; Arvia, A. J. *J. Electroanal. Chem.* **1993**, *357*, 339.
- (4) Vaskevich, A.; Rosenblum, M.; Gileadi, E. *J. Electroanal. Chem.* **1995**, *383*, 167.
- (5) Aberdam, D.; Salem, C.; Durand, R.; Faure, R. *Surf. Sci.* **1990**, *239*, 71.
- (6) Marinkovic, N. S.; Wang, J. X.; Adzic, R. R. *Proc. Electrochem. Soc.* **1997**, *97* (17), 251.
- (7) Wang, J. X.; Marinkovic, N. S.; Adzic, R. R.; Ocko, B. *Surf. Sci.* **1998**, *398*, L291.
- (8) Roder, H.; Schuster, R.; Brune, H.; Kern, K. *Phys. Rev. Lett.* **1993**, *71*, 2086.
- (9) Kimizuka, N.; Itaya, K. *Faraday Discuss.* **1992**, *94*, 117.
- (10) Wang, J.; Ocko, B. M.; Davenport, A. J.; Isaacs, H. S. *Phys. Rev. B* **1992**, *46*, 10321.
- (11) Marinkovic, N. S.; Hecht, M.; Loring, J. S.; Fawcett, W. R. *Electrochim. Acta* **1996**, *41*, 641.
- (12) Marinkovic, N. S.; Marinkovic, J. S.; Adzic, R. R. *J. Electroanal. Chem.*, in press.
- (13) Stole, S. M.; Popoenoe, D. D.; Porter, M. D. In *Electrochemical Interfaces: Modern Techniques for In situ Interface Characterization*; Abruna, H. D., Ed.; VCH Publishers: New York, 1991 and references therein.
- (14) Blyholder, G. *J. Phys. Chem.* **1964**, *68*, 2772.
- (15) Marinkovic, N. S.; Hecht, M.; Andreu, R.; Fawcett, W. R. *J. Phys. Chem.* **1995**, *99*, 6760.
- (16) Iwasita, T.; Xia, X. *J. Electroanal. Chem.* **1996**, *411*, 95.
- (17) Faguy, P. W.; Marinkovic, N. S.; Adzic, R. R. *Langmuir* **1996**, *12*, 243.
- (18) Nakamoto, K. *Infrared and Raman Spectra of Inorganic and Coordination Compounds*, 5th ed.; J. Wiley and Sons: New York, 1997.
- (19) Faguy, P. W.; Marinkovic, N. S.; Adzic, R. R. *J. Electroanal. Chem.* **1996**, *407*, 209.
- (20) Mrozek, P.; Han, M.; Sung, Y. E.; Wieckowski, A. *Surf. Sci.* **1994**, *319*, 21.
- (21) Patrito, E. M.; Olivera, P. P.; Sellers, H. *Surf. Sci.* **1997**, *380*, 264.
- (22) Smolinski, S.; Zelenay, P.; Sobkowski, J. *J. Electroanal. Chem.* **1998**, *442*, 41.
- (23) Paffett, M. T.; Campbell, C. T.; Taylor, T. N.; Srinivasan, S. *Surf. Sci.* **1985**, *154*, 284.
- (24) Shek, M. L.; Stefan, P. M.; Lindau, I.; Spicer, W. E. *Phys. Rev. B* **1983**, *27*, 7277.
- (25) Rodriguez, J. A.; Kuhn, M. *J. Phys. Chem.* **1994**, *98*, 11251.
- (26) Hanson, W.; Bertolo, M.; Jacobi, K. *Surf. Sci.* **1991**, *253*, 1.
- (27) Rodriguez, J. A.; Truong, C. M.; Goodman, D. W. *Surf. Sci. Lett.* **1992**, *271*, L331.
- (28) Oda, I.; Ogasawara, H.; Ito, M. *Langmuir* **1996**, *12*, 1094.
- (29) Bewick, A. *J. Electroanal. Chem.* **1983**, *150*, 481.